CERN-INTC-2022-006 / INTC-I-240
05/01/2022

EUROPEAN ORGANIZATION FOR NUCLEAR RESEARCH

Letter of Intent to the ISOLDE and Neutron Time-of-Flight Committee

Development of neutron-deficient Ba beams for a systematic study approaching the $N = Z = 56$ ^{112}Ba

January 5, 2022

A. Illana[1,2], J.J. Valiente-Dobón[3], G. de Angelis[3], A. Briscoe[1,2], M.J.G. Borge[4], J.A. Briz[5], P.A. Butler[6], L.M. Fraile[5], L.P. Gaffney[6], A. Gottardo[3], A. Goasduff[3], P. Greenlees[1,2],R. Heinke[7], D. Mengoni[8], A. Montes-Plaza[1,2,6], E. Nácher[9], J. Ojala[1,2], B. Olaizola[7], J. Pakarinen[1,2], R.M. Pérez-Vidal[3], P. Ruotsalainen[1,2], S. Rothe[7], S. Stegemann[7], D. Stramaccioni[3], M. Stryjczyk[1,2], O. Tengblad[4], A. Tolosa-Delgado[1,2], M. Zielińska[10], G.L. Zimba[1,2] and the ISOLDE Target + RILIS Group

[1] *Accelerator Laboratory, University of Jyväskylä, Jyväskylä, Finland.*

[2] *Helsinki Institute of Physics, Helsinki, Finland.*

[3] *Istituto Nazionale di Fisica Nucleare, Laboratori Nazionali di Legnaro, Legnaro, Italy.*

[4] *Instituto de Estructura de la Materia, CSIC, Madrid, Spain.*

[5] *Universidad Complutense, Grupo de Física Nuclear and IPARCOS, CEI Moncloa, Madrid, Spain.*

[6] *Department of Physics, Oliver Lodge Laboratory, University of Liverpool, Liverpool, UK.*

[7] *ISOLDE, CERN, Switzerland.*

[8] *Dipartimento di Fisica e Astronomia dell'Universit, and INFN, Sezione di Padova, Padova, Italy.*

[9] *Instituto de Física Corpuscular, CSIC and Universidad de Valencia, Paterna, Spain.*

[10] *IRFU, CEA, Universitè Paris-Saclay, Gif-sur-Yvette, France.*

Spokesperson: Andres Illana [andres.illana@cern.ch] and
Jose Javier Valiente-Dobón [Javier.Valiente@lnl.infn.it]
Contact person: Sebastian Rothe [Sebastian.Rothe@cern.ch] and
Reinhard Heinke [reinhard.heinke@cern.ch]

Abstract: This Letter of Intent (LoI) proposes the development of barium beams at ISOLDE to perform future Coulomb excitation experiments of neutron-deficient barium isotopes. Enhanced octupole correlations are expected in the $N \simeq Z$ nuclei just above ^{100}Sn, but experimental evidence is presently scarce. In this region, the strongest octupole correlations are expected for the $N = Z = 56$ ^{112}Ba, but this nucleus is currently out of reach in experiments with stable beams and targets. The aim of this Letter of Intent is the measurement of the yields and isobaric contaminations of the $^{114-120}$Ba isotopes. This initial measurement will help us to assess the feasibility of future experiments with the objective of a systematic measurement of the octupole correlations in these light barium isotopes.

Requested shifts: 6 shifts split into [1] runs over [1] years.

1 Motivation

The existence of nuclei with stable deformed shapes was discovered early in the history of nuclear physics. The observation of large quadrupole moments led to the suggestion that some nuclei might have spheroidal shapes, which was confirmed by the observation of rotational band structures. The main shapes, spherical, oblate and prolate, arise from the quadrupole deformation with axial and reflection symmetry. Since such a shape is symmetric under space inversion, all members of the rotational band will have the same parity. Instead, nuclei that present a reflection-asymmetric shape, as for example pear shape, will develop low-lying negative-parity states. Extensive investigations of these kinds of deformations have concluded that they are not as stable as the familiar quadrupole deformations. Octupole correlations are generated microscopically by the interaction between orbitals of opposite parity near the Fermi surface, which differ by three units of angular momentum. In general, this situation occurs when the Fermi level lies between an intruder-orbital and the normal parity subshell. These correlations happen in well-defined areas of the Segrè chart, when the number of protons or neutrons is equal to 34, 56, 88 and 134 [1, 2]. And hence, islands of octupole-deformed nuclei can be defined as regions where two octupole magic numbers intersect.

Currently, octupole correlations around the ^{144}Ba (Z = 56 and N = 88) [3, 4] and ^{220}Ra [3, 5–7] (Z = 88 and N = 132) nuclei have been extensively investigated in the last decade. Nonetheless, nuclei around ^{112}Ba (N = Z = 56), in particular between $50 \leq Z \leq 56$ and $54 \leq N \leq 60$, represent an experimental challenge and still nowadays very little is known beyond N = 56 for Te, Xe and Ba isotopes, see Figure 1.

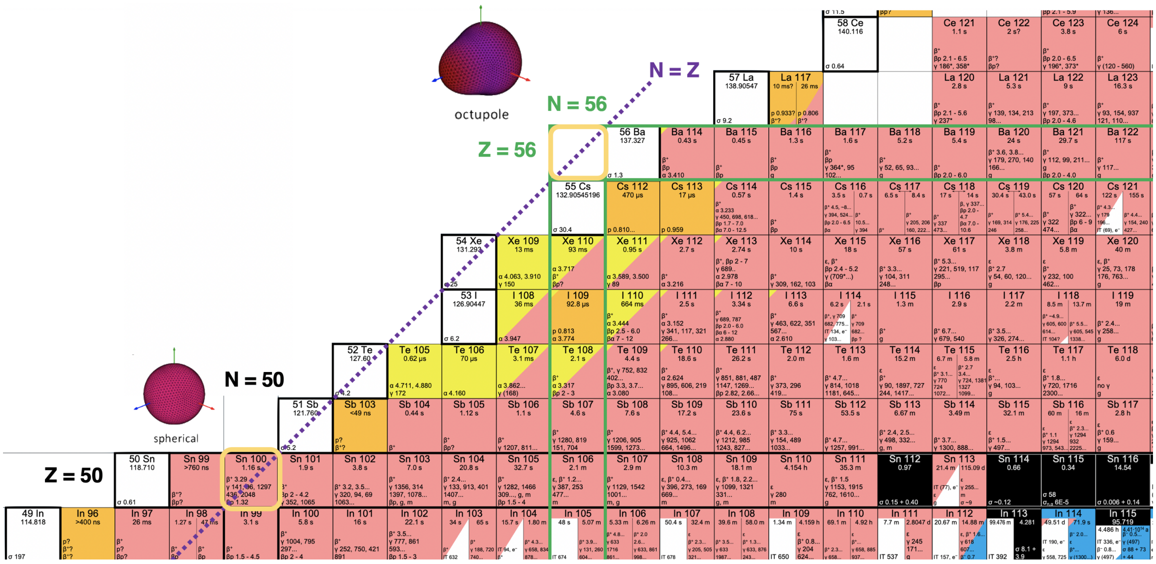

Figure 1: Region of interest in the Segrè chart.

Nowadays, the only existent information around this region was obtained in stable facilities via fusion-evaporation reactions. Presently, for the even-even neutron deficient barium nuclei only the ground-state band and a negative-parity band have been identified in ^{118}Ba and ^{120}Ba [8, 9]. Actually, only for ^{114}Xe the reduced transition probability for the 3^- to 0^+ state, B(E3), has been measured to be 77 (27) W.u., which is one of the largest octupole strengths that have ever been experimentally measured [10]. However, the strongest octupole is supposed to happen for ^{112}Ba, but that has currently never been observed. There is presently no known spectroscopic information for the lighter even-even barium isotopes with A<118. However, the $^{114-116}$Ba nuclei have been the subject of several decay studies, as described in Ref. [11–13].

Currently, a few theoretical studies on the octupole deformation around Z = 56 have been published [14–17]. In particular, we would like to mention the recent calculations from *Nomura et al.* [15]. Here, the authors analyse octupole deformations and related collective excitations using the framework of nuclear density functional theory. For this purpose, axially symmetric quadrupole-octupole constrained self-consistent mean-field (SCMF) calculations with a choice of universal energy density functional and a pairing interaction were performed for the isotopic chain of Xe, Ba, and Ce isotopes. Collective states were described using an axially symmetric Quadrupole-Octupole Collective Hamiltonian (QOCH). More details about the theory can be found in Ref. [15]. The main results of the calculations for the Ba isotopes are shown in Fig. 2.

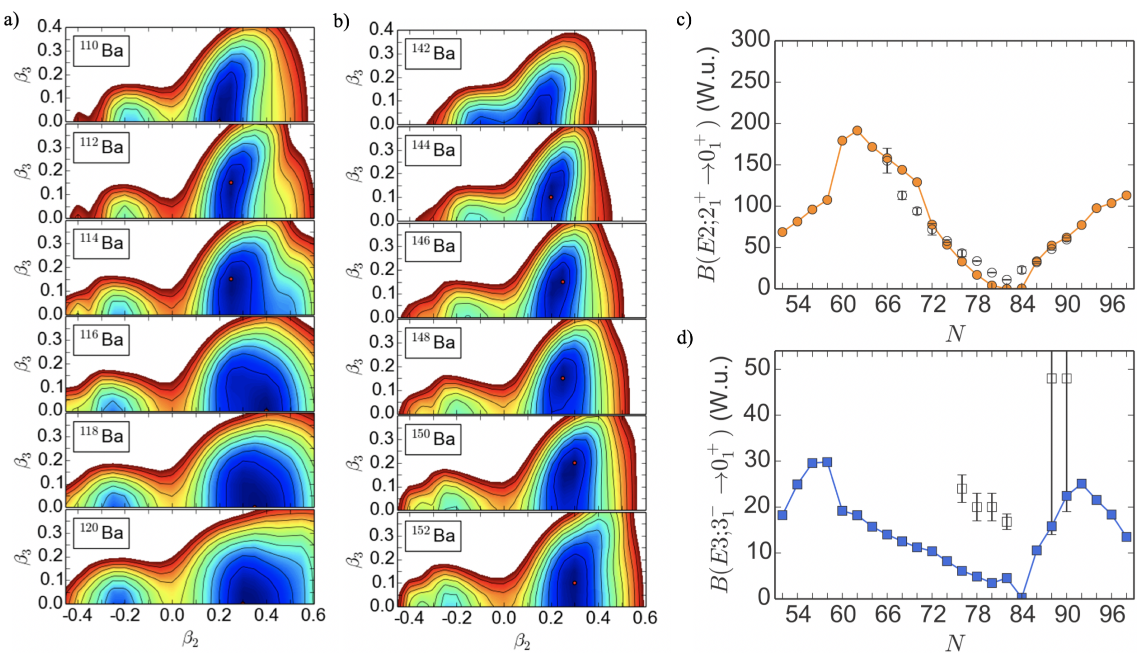

Figure 2: Results of theoretical calculations as described in the text. SCMF (β_2, β_3) PESs for a) $^{110-120}$Ba, and b) $^{142-152}$Ba. Global minima are identified by the red dots. Contours join points on the surface with the same energy, and the difference between neighboring contours is 1 MeV. c) $B(E2;\ 2_1^+ \to 0_1^+)$ and d) $B(E3;\ 3_1^- \to 0_1^+)$ reduced transition probabilities for the Ba isotopes. Solid symbols connected by lines denote the QOCH results. Experimental values (open symbols) are taken from the ENSDF database [18]. All the figures were extracted from Ref. [15]. Results of theoretical calculations as described in the text.

The axially symmetric (β_2, β_3) Potential Energy Surfaces (PESs) for neutron-deficient nuclei $^{110-120}$Ba and neutron-rich nuclei $^{142-152}$Ba are presented in Fig 2.a) and Fig 2.b), respectively. It is clear that the global minima, see the red dots, behaves very different between both regions, N = 56 and N = 88. For the most neutron deficient side, PESs are considerably soft in β_3 deformation and octupole deformed equilibrium states with $\beta_3 \neq 0$ occur in ^{112,114}Ba. On the other hand, the neutron-rich Ba isotopes are more rigid in β_2, and pronounced octupole correlations are predicted in this case. Almost all the neutron-rich Ba nuclei presented here exhibit an octupole-deformed global minima with nonzero value of β_3.

The results for the $B(E2;\ 2_1^+ \rightarrow 0_1^+)$ and d) $B(E3;\ 3_1^- \rightarrow 0_1^+)$ reduced transition probabilities along the Ba isotopic chain are shown in Fig 2.c) and Fig 2.d), respectively. There is a clear agreement between the experimental B(E2) values and the calculations. However, the theoretical $B(E3)$ values are systematically underestimated respect to the few experimental known values in the neutron-rich side. In both cases the calculation predicts two maxima, one at N $\approx$ 56 and the other at N $\approx$ 88.

In summary, in order to have a better understanding of the quadrupole and octupole correlations around N = Z = 56 and to improve the existing theoretical models, it is imperative to provide reliable experimental data.

2 Future experiments

The present lack of experimental information about the excited states and transition probabilities in the very neutron-deficient barium isotopes can be addressed by exploiting recent experimental beam developments at ISOLDE. Our final aim is to perform several safe Coulomb Excitation (Coulex) experiments along the even-even neutron-deficient Ba isotopes. For this purpose, the Miniball array coupled with the standard CD detector or the C-REX detector have proven to be a very powerful tool for measuring quadrupole and octupole moments of a wide variety of nuclei at ISOLDE [19, 20]. In order to perform a Coulex analysis, the ions of interest will be impinging on a heavy target such as ^{208}Pb or ^{196}Pt and the beam energies should be between 4.0-4.4 MeV/u depending on the beam and target combination. More details about the experimental setup will be supplied in a proper proposal.

3 Beam development

Neutron-deficient Ba isotopes have been produced and tested before the first long shutdown [21] using, at that time, a recently made LaC_2 target. During that experiment, a large isobaric Cs contamination was observed. Therefore, molecular beams using a fluorine gas were used to separate Ba from Cs. Unfortunately, due to some problems in the target the most exotic Ba yield measured was ^{118}Ba with a production of $2 \cdot 10^5$ ions/μC [22, 23]. More details can be found in the status report of the IS545 experiment [24].

Recently a new type of target has been developed to address the high degree of isobaric surface ionization contamination, as it is expected in this region. The Laser Ion Source and Trap (LIST) target is able to suppress surface ionized isobaric contaminants using a repelling electrode and at the same time to ionise the elements of interest via laser ionisation [25, 26]. However, the LIST mode is less efficient than the RILIS mode, but for each case this scaling factor has to be measured. In a recent test, a conservative suppression factor of 10^3 have been obtained using UC_x targets with this new mode of operation. In addition, a Ba laser ionization scheme is already available as indicated in the RILIS database [27]. It is important to mention that currently ISOLDE has a plan to perform yield measurements in the neutron-rich Ba isotopes using a LIST unit with a UC_x target [28]. For a strongly surface-ionized species such as Ba, a higher loss factor might occur in using LIST as the fraction remaining neutral and being available for laser ionization is significantly reduced. The influence of the transfer line heating needs to be investigated in this context. Hence, the yield production and isobaric contamination for each light Ba isotopes will be measured using different extraction modes: only surface ionized, RILIS assisted and LIST mode. In summary, this LoI represents a natural extension of the current development plan of yield measurements at ISOLDE for the heavy Ba isotopes using UC_x target to the light Ba isotopes using the LaC_2 target. The yield measurements and determination of release curves can be done at the ISOLDE tape station, as it is programmed for the neutron-rich Ba isotopes.

Summary of requested shifts: We request 6 shifts in total for the $^{114-120}$Ba isotopes.

References

[1] P.A. Butler and W. Nazarewicz. *Review of Modern Physics*, 68:349–421 (1996).

[2] P.A. Butler. *Journal of Physics G: Nuclear and Particle Physics*, 43:073002 (2016).

[3] B. Bucher, et al. *Physical Review Letters*, 116:112503 (2016).

[4] B. Bucher, et al. *Physical Review Letters*, 118:152504 (2017).

[5] L.P. Gaffney, et al. *Nature*, 497:199–204 (2013).

[6] P.A. Butler, et al. *Nature Communications*, 10:2473 (2019).

[7] P. A. Butler, et al. *Physical Review Letters*, 124:042503 (2020).

[8] J.F. Smith, et al. *Physical Review C*, 57:R1037–R1041 (1998).

[9] J.F. Smith, et al. *Physics Letters B*, 483:7–14 (2000).

[10] G. de Angelis, et al. *Physics Letters B*, 535:93–102 (2002).

[11] Z. Janas, et al. *Nuclear Physics A*, 627:119–136 (1997).

[12] C. Mazzocchi, et al. *Physics Letters B*, 532:29–36 (2002).

[13] L. Capponi, et al. *Physical Review C*, 94:024314 (2016).

[14] R.N. Bernard, L.M. Robledo, and T.R. Rodríguez. *Physical Review C*, 93(6):061302R (2016).

[15] K. Nomura, et al. *Phys. Rev. C*, 103:054301 (2021).

[16] K. Nomura, R. Rodríguez-Guzmán, and L.M. Robledo. *Physical Review C*, 104:054320 (2021).

[17] R. Rodríguez-Guzmán, et al. *Journal of Physics G: Nuclear and Particle Physics*, 49:015101 (2022).

[18] National Nuclear Data Center (NNDC). *http://www.nndc.bnl.gov* (2021).

[19] N. Warr, et al. *The European Physical Journal A*, 49(3):40 (2013).

[20] P. Reiter and N. Warr. *Progress in Particle and Nuclear Physics*, 113:103767, 2020.

[21] J. Ray, et al. *INTC: IS545 proposal* (2012).

[22] The ISOLDE Yields database. *https://isoyields2.web.cern.ch/* (2021).

[23] S. Rothe. *Private communication* (2021).

[24] J. Ray, et al. *INTC: IS545 Starus report* (2014).

[25] D.A. Fink, et al. *Nuclear Instruments and Methods in Physics Research Section B: Beam Interactions with Materials and Atoms*, 344:83 – 95 (2015).

[26] D. A. Fink, et al. *Phys. Rev. X*, 5:011018 (2015).

[27] The ISOLDE RILIS. *https://rilis-web.web.cern.ch* (2021).

[28] R. Heinke. *Private communication* (2021).

Appendix

DESCRIPTION OF THE PROPOSED EXPERIMENT

The experimental setup comprises: Yield Measurements.

Part of the	Availability	Design and manufacturing
Yield Measurements	☒ Existing	☒ To be used without any modification

HAZARDS GENERATED BY THE EXPERIMENT (if using fixed installation:) Hazards named in the document relevant for the fixed [MINIBALL + only CD, MINIBALL + T-REX] installation.

Additional hazards:

Hazards	[Part 1 of experiment/ equipment]	[Part 2 of experiment/ equipment]	[Part 3 of experiment/ equipment]
Thermodynamic and fluidic			
Pressure	[pressure][Bar], [volume][l]		
Vacuum			
Temperature	[temperature] [K]		
Heat transfer			
Thermal properties of materials			
Cryogenic fluid	[fluid], [pressure][Bar], [volume][l]		
Electrical and electromagnetic			
Electricity	[voltage] [V], [current][A]		
Static electricity			
Magnetic field	[magnetic field] [T]		
Batteries	☐		
Capacitors	☐		
Ionizing radiation			
Target material [material]			
Beam particle type (e, p, ions, etc)			
Beam intensity			
Beam energy			
Cooling liquids	[liquid]		
Gases	[gas]		
Calibration sources:	☐		
• Open source	☐		

• Sealed source	☐ [ISO standard]		
• Isotope			
• Activity			
Use of activated material:			
• Description	☐		
• Dose rate on contact and in 10 cm distance	[dose][mSV]		
• Isotope			
• Activity			
Non-ionizing radiation			
Laser			
UV light			
Microwaves (300MHz-30 GHz)			
Radiofrequency (1-300 MHz)			
Chemical			
Toxic	[chemical agent], [quantity]		
Harmful	[chem. agent], [quant.]		
CMR (carcinogens, mutagens and substances toxic to reproduction)	[chem. agent], [quant.]		
Corrosive	[chem. agent], [quant.]		
Irritant	[chem. agent], [quant.]		
Flammable	[chem. agent], [quant.]		
Oxidizing	[chem. agent], [quant.]		
Explosiveness	[chem. agent], [quant.]		
Asphyxiant	[chem. agent], [quant.]		
Dangerous for the environment	[chem. agent], [quant.]		
Mechanical			
Physical impact or mechanical energy (moving parts)	[location]		
Mechanical properties (Sharp, rough, slippery)	[location]		
Vibration	[location]		
Vehicles and Means of Transport	[location]		
Noise			
Frequency	[frequency],[Hz]		
Intensity			

Physical			
Confined spaces	[location]		
High workplaces	[location]		
Access to high workplaces	[location]		
Obstructions in passageways	[location]		
Manual handling	[location]		
Poor ergonomics	[location]		

Hazard identification:

Average electrical power requirements (excluding fixed ISOLDE-installation mentioned above): [make a rough estimate of the total power consumption of the additional equipment used in the experiment]: ... kW